Journal of Engineering and Technology for Industrial Applications

ISSN ONLINE: 2447-0228

ITEGAM-JETIA

Manaus, v.12 n.58, p. 575-588. March/April, 2026.
DOI: https://doi.org/10.5935/jetia. v12i58.3184

RESEARCH ARTICLE OPEN ACCESS

EVALUATION OF METHYLENE BLUE REMOVAL USING A FOOD-INDUSTRY BYPRODUCT VIA SIMULATION AND MODELING

Salah Eddine Bencheikh*[1, 4], Mohamed Bilal Goudjil[2] and Ladjel Segni[3]

[1, 2, 3]Laboratory of Process Engineering, Faculty of Applied Sciences, Kasdi Merbah University, Ouargla POB 511 Ouargla, Algeria
[4]University of Ghardaia, POB 455 Ghardaia, Algeria

[1]https://orcid.org/0000-0002-3235-348X, [2]https://orcid.org/0000-0001-8125-4405, [3]https://orcid.org/0000-0002-6016-9428

Email: Bencheikh.salah@gmail.com, gdbilal@yahoo.fr, ladjejsegni@yahoo.fr

ARTICLE INFO

Article History
Received: December 22, 2025
Reviewed: January 9, 2026
Accepted: January 16, 2026
Published: March 31, 2026

Keywords:
Food waste,
Adsorbent,
Methylene blue,
Adsorption,
Mathematical model.

ABSTRACT

Our work examines the use of peanut shells, a common and cheap food waste, as a natural adsorbent for treating industrial dyes, particularly methylene blue in this study. We also performed a comprehensive analysis of adsorption, which showed that it follows both Langmuir and Freundlich adsorption isotherms, signifying that peanut shells are efficient adsorbents for methylene blue. To enhance the outcome of the adsorption, a Box-Behnken design was used in our experiment. This design enabled us to examine how various important parameters, such as the amount of adsorbent, concentration of the dye, pH, temperature, rate of stirring, and the ionic strength of dissolved salts, can affect this procedure. Also, a mathematical model and simulation of this adsorption reaction enabled us to find optimal conditions for efficient removal of this dye. In our experiments, the highest adsorption efficiency of 97% was obtained under optimal conditions of 1.5g of adsorbent, a concentration of 40mg/L of MB, a pH of 11, a temperature of 65°C, 0 mg/L ionic strength, and a stirring speed of 165 rpm. These results reveal that peanut shells can be considered a potential, environmentally sustainable alternative for removing dyes.

I. INTRODUCTION

With the growth of humanity and the advancement of science and technology, the world reaches new horizons; however, this rapid growth will carry high costs in the near future. One of its major consequences is environmental degradation, particularly the growing problem of pollution. Water and soil contamination by industrial chemicals including dyes, heavy metals, phenolic compounds, pesticides, and fertilizers are a source of serious environmental impairment internationally. Organic dyes being resistant to biodegradation with accumulation and high levels of industrial applications, especially in textile industries, possess a high threat potential for environmental and human health[1].

These synthetic dyes also have widespread use in the paper, cosmetic, and food industries as well [2]. Several treatment methods such as adsorption, filtration, coagulation, flocculation, and membrane separation have been developed to mitigate these pollutants. Of these, adsorption is acknowledged as one of the effective and simple processes for organic contaminant removal, especially when low-cost or abundant natural adsorbents are made from waste materials [1]. In the present study, peanut shell wastes, one of the most abundant wastes, were used as a low-cost adsorbent material for the removal of methylene blue, which was selected as a representative organic dye based on its extensive use in various industries.

II. MATERIALS AND METHODS

II.1 PEANUT SHELL (PS) PREPARATION PROCESSES

II.1.1 Washing

First, peanut shells were crushed using a mortar in order to obtain smaller fragments. Ten grams of this crushed material were soaked into 1 liter of distilled water for 15 minutes.

After that, it was subjected to manual stirring to ensure good contact and the improvement of interactions between solid and liquid phases. Then, the sample was filtered through a simple strainer and washed with distilled water. This washing was repeated eight times until the filtrate became transparent and free of turbidity.

II.1.2 Drying

The cleaned peanut shells were cut into small pieces and left to air-dry. They were oven-dried at 50-60°C for 24 hours to remove the moisture completely.

II.2 PREPARATION OF THE "ADSORBATE" SOLUTION

A stock solution of methylene blue (100 mg/L) was prepared and stored in the dark to prevent degradation. Serial dilutions were performed to obtain the required working concentrations. All weighings necessary for the preparation of the solutions were conducted using a precision analytical balance.

II.2.1 Calibration Curves

The calibration curve, generated from diluted dye solutions at λmax =664nm, exhibited strong linearity between absorbance (Abs) and concentration (C), confirming the method's suitability for dye analysis.

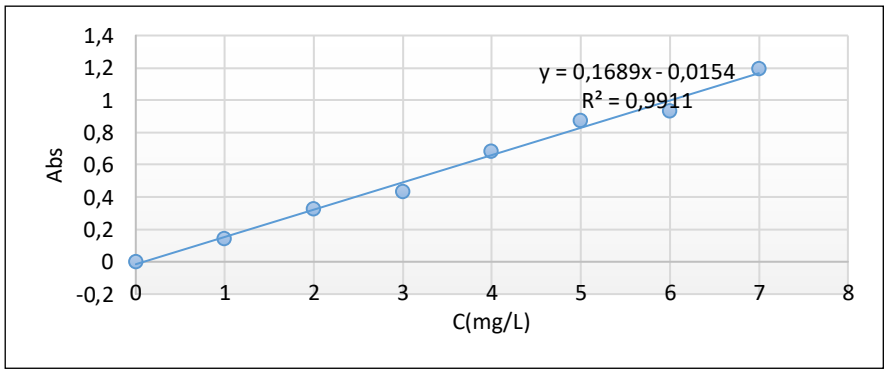

Figure 1: Calibration curve of MB at λmax =664nm.
Source: Authors, (2026).

II.3 CALCULATION FORMULAS

To determine the residual concentrations of MB in the liquid phase at time t, the linear equation is applied:

$$Y = 0.1689\,X - 0.0154 \quad (1)$$

where:
Y: the absorbance (A) at time t.
X: the residual concentration of MB at time t.
To calculate the quantity of biosorbed MB q_t (mg/g) at time t:

$$q_t = \frac{(C_0 - C_t)\times V}{m} \quad (2)$$

where:
C_0: The initial concentration (at t=0) of biosorbed MB in the liquid phase(mg/l).
C_t : The concentration of MB at time T in the liquid phase.
m: Mass of dry biosorbent (g).
To calculate the quantity of MB at equilibrium q_e (mg/g), the following formula is used:

$$q_e = \frac{(C_0 - C_e)\times V}{m} \quad (3)$$

where:
C_e : The concentration of MB in the aqueous phase at equilibrium (mg/L).
V: Volume of the solution (L).
To calculate the removal efficiency of MB at time t (%), the following formula is applied:

$$R(\%) = \frac{(C_0 - C_t)}{C_0} \quad (4)$$

To calculate the change in concentration of MB after the adsorption phenomenon, the following formula is applied:

$$\Delta C = c_0 - c_e \quad (5)$$

where: ΔC : The change in concentration (mg/L).

II.4. OPTIMIZATION

II.4.1 Experimental Designs

Experimental designs allow for the optimal organization of trials in both scientific and industrial studies. They are widely applicable across disciplines and industries where the goal is to understand the relationship between a response variable, Y, and explanatory variables, X_i. These designs are particularly valuable when the aim is to explore a function of the form: $Y = f(X_i)$ [3].

II.4.1.1 The Studied Factors

Table 1: Levels of the Studied Factors.

Levels	$C(BM)(mg/l)$	m (*Waste*) (g)	pH	$T(^0C)$	$C(NaCl)$(mg/l)	Stirring speed (rpm)
-1	5	0,2	2	30	0	0
0	22.5	0.85	6.5	47.5	0.05	115
$+1$	40	1,5	11	65	0.1	230

Source: Authors, (2026).

II.4.1.2 Measured Responses

Table 2: Measured Responses.

N	(1)	(2)	(3)
Responses	$Qm\ (mg/g)$	$\Delta C\ (mg/L)$	R (%)

Source: Authors, (2026).

II.4.1.3 Box-Behnken Design

In 1960, Box and Behnken introduced experimental designs that directly establish second-degree models. Each factor in these designs is evaluated at three levels: -1, 0, and +1. These designs are user-friendly and possess a sequential nature, allowing researchers to start with an initial set of factors and later add more without compromising previous results. The Box-Behnken design for three factors is depicted as a cube with 12 edges, typically including three central points in the study domain. Thus, the design involves 12 edge points plus 3 central experiments, totaling 15 experiments. [4]. The first experimental design measures two responses: Q_m and ΔC, while considering three factors: concentration (C), pH, and the mass of the peanut shell. The second experimental design focuses on yield (R) and examines three factors: temperature, ionic strength (NaCl concentration), and stirring speed (VA).

III. RESULTS AND DISCUSSION

III.1 EFFECT OF INITIAL CONCENTRATION

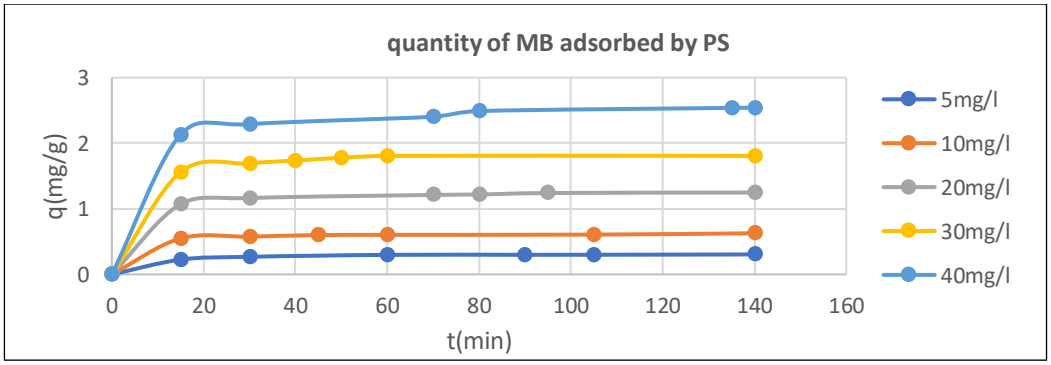

Figure 2: The effect of initial concentration on MB adsorption.
Source: Authors, (2026).

The sorption capacity of the biosorbent rises with increasing time, which shows that methylene blue [2] sorption depends upon the initial concentration. The dynamic equilibrium for MB adsorption takes place after a period of one hour, with higher MB adsorption as the initial concentration of MB becomes higher. The initial period of rapid adsorption takes place in the initial 50 min, where many adsorption sites are available on the surface of the adsorbent. With increasing time, longer periods are needed for diffusion of the molecules into the pores of the adsorbent, while the remaining amount that is not adsorbed is due to surface saturation of sites.

III.2 MODELING OF ADSORPTION ISOTHERM EQUILIBRIA

The Langmuir and Freundlich equations are employed to model adsorption isotherm equilibria. These equations accurately relate experimental data and provide insight into the adsorption reaction.

III.2.1 Langmuir Model

The modeling of the experimental results of the MB adsorption isotherm by PS using the Langmuir equation is presented in the following curve: $\mathbf{1/q_e = f(1/C_e)}$**……. (6)**

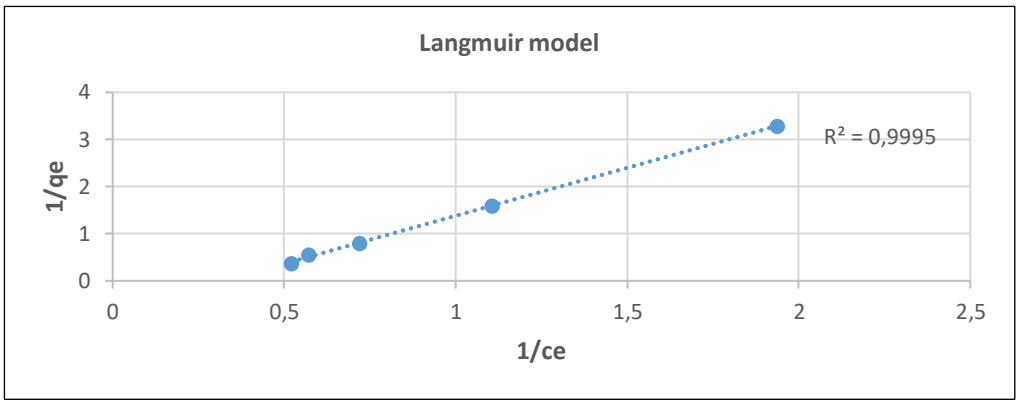

Figure 3: Modeling of the MB Adsorption Isotherm by PS using the Langmuir Equation.
Source: Authors, (2026).

According to the curve, we have:

$$1/q_e = 2.0344(1/C_e) - 0.6531 \quad (7)$$

III.2.2 Freundlich Model

The modeling of methylene blue [2] adsorption onto peanut shells (PS) using the Freundlich isotherm is illustrated in the accompanying curve. The correlation coefficients (R^2) obtained from the Langmuir and Freundlich models are 0.999 and 0.98, respectively. Although both models are suitable, the Langmuir model offers a better fit for the experimental data of MB adsorption.

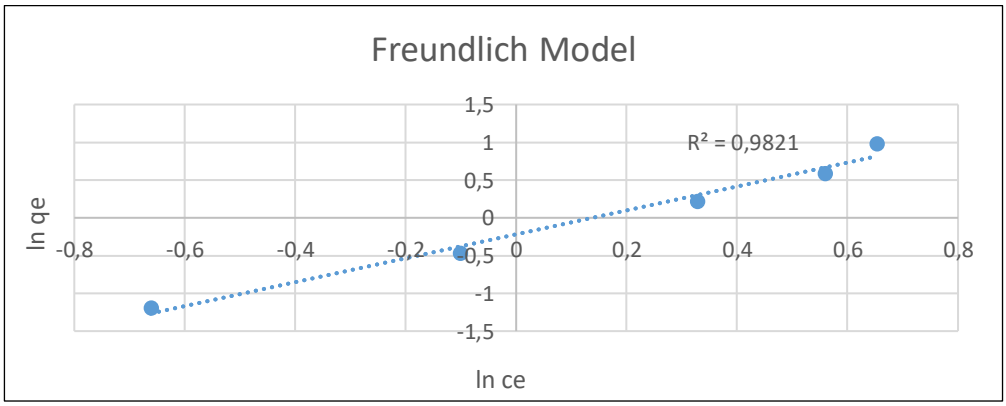

Figure 4: Modeling of the MB Adsorption Isotherm by PS using the Freundlich Equation.
Source: Authors, (2026).

Adsorption isotherms enable the analysis of the equilibrium behavior of methylene blue [2] and offer insights into the mechanisms involved in the adsorption process. Several models, including first-order and second-order kinetic models, are documented in the literature to describe adsorption kinetics.

III.3 ADSORPTION KINETICS OF MB

III.3.1 First-Order Kinetic Model

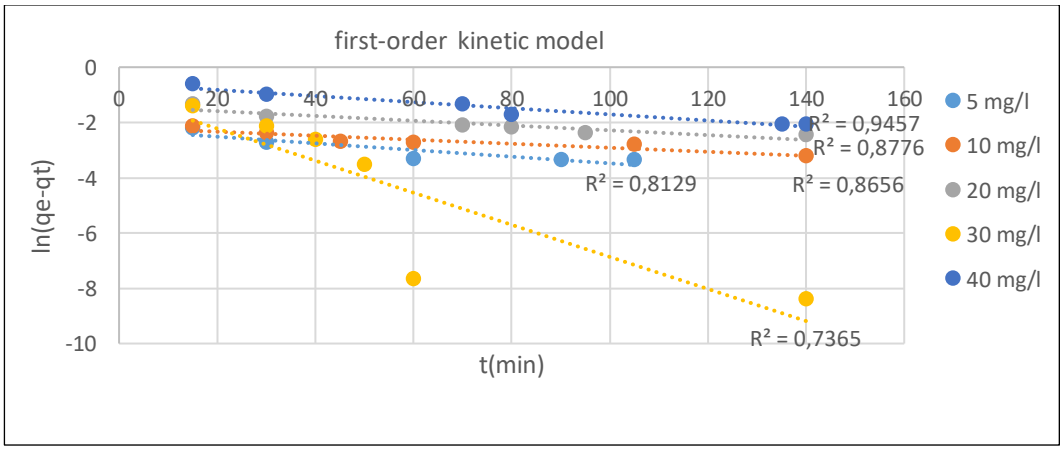

Figure 5: First-order kinetic model.
Source: Authors, (2026).

III.3.2 Second-ORDER KINETIC MODEL

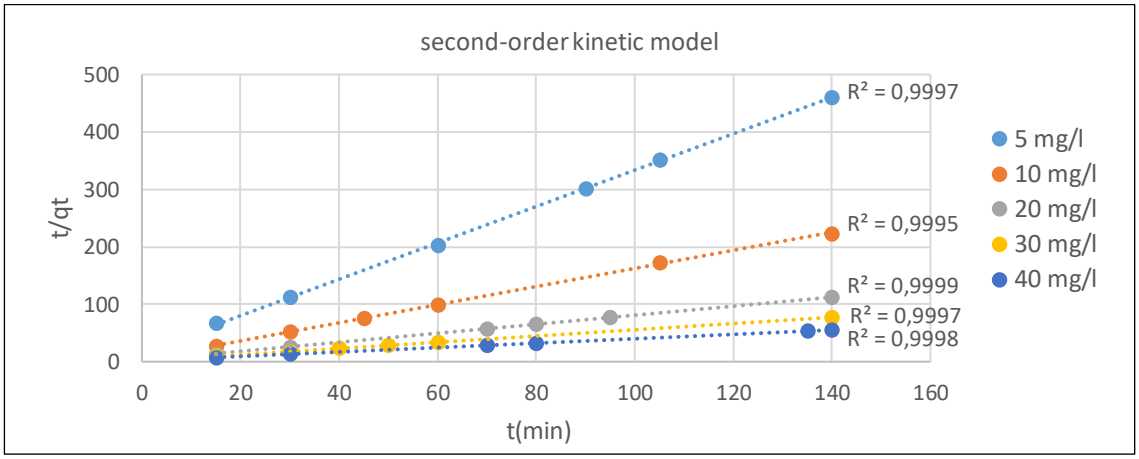

Figure 6: Second-order kinetic model.
Source: Authors, (2026).

The results indicate that the correlation coefficients for the pseudo-first-order and pseudo-second-order kinetic models demonstrate that the adsorption kinetics are best described by the pseudo-second-order model for the studied adsorbent.

III.4 OPTIMIZATION OF MB ADSORPTION

The regression coefficients were calculated using coded data in MINITAB software version 19, and the response surface was generated using Design Expert software version 11.

III.4.1 Response Analysis of Qm

The first experimental design: Analysis of the Response Qm

III.4.1.1 Analysis of Variance (ANOVA)

Table 3: Estimated Regression Coefficients for Qm (Current Unit).

Source	DF	Adjus Sum of Squares	CM adjust	F-value	P-value
Model	9	149,633	16,6259	13,42	0,005
Linear	3	112,078	37,3594	30,15	0,001
C	1	39,765	39,7648	32,10	0,002
m	1	70,248	70,2479	56,70	0,001
pH	1	2,066	2,0656	1,67	0,253
Square Terms	3	19,210	6,4033	5,17	0,054
C^2	1	0,668	0,6676	0,54	0,496
m^2	1	17,886	17,8864	14,44	0,013
pH^2	1	0,020	0,0200	0,02	0,904
Two-Factor Interaction Terms	3	18,345	6,1150	4,94	0,059
C×m	1	16,824	16,8238	13,58	0,014
C×pH	1	0,748	0,7484	0,60	0,472
m×pH	1	0,773	0,7727	0,62	0,465
Error	5	6,195	1,2389		
Lack of Fit	3	6,194	2,0646	4477,72	0,000
Pure Error	2	0,001	0,0005		
Total	14	155,828			

Source: Authors, (2026).

Table 4: Model Summary.

S	R Square	R Square (Adjus)	R Square (Predi)
0,967547	94,59%	91,59%	76,14%

Source: Authors, (2026).

According to Table 3, the model exhibited high significance with a very low p-value (p = 0.005), as shown by the ANOVA for the regression models. Additionally, the linear effects, with a p-value of 0.001, indicate a significant influence of the main factors (C and m) on conversion. A significant interaction effect was also observed for C × m. The ANOVA results in Table 7 show a determination coefficient of R^2 = 94.59% and an adjusted R^2 = 91.59%, both close to 1, indicating a strong model fit to the actual system. Furthermore, the predicted R^2 = 76.14% demonstrates a good correlation between measured and predicted values. The effects are further illustrated in the accompanying Pareto chart.

III.4.1.2 Regression Equation In Uncoded Units

The analysis of variance (ANOVA), after excluding non-significant terms, indicates that all remaining terms are highly significant. This confirms that the refined model is statistically superior.

$$Qm = 2{,}60 + 0{,}2806\ C - 9{,}46\ m + 0{,}1129\ pH + 5{,}27\ m^2 - 0{,}1803\ C \times m$$

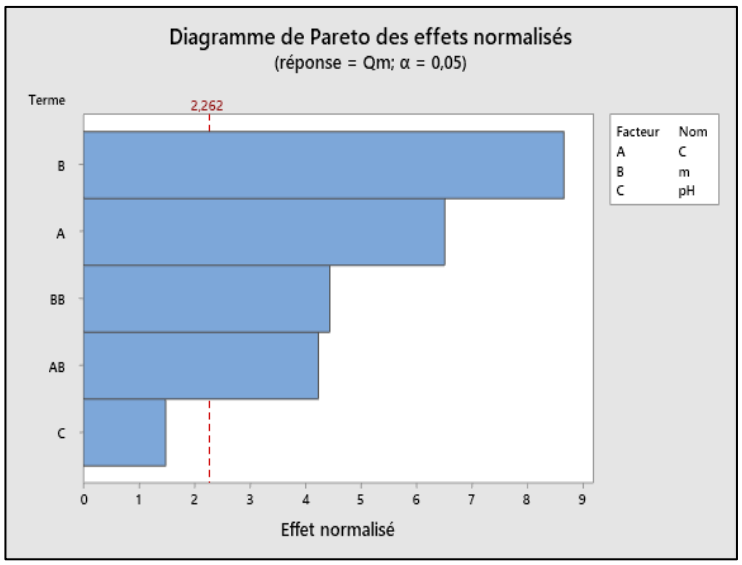

Figure 7: Pareto Chart of Normalized Effects for the Response Qm.
Source: Authors, (2026).

III.4.1.3 Main Effects and Interactions Affecting Qm

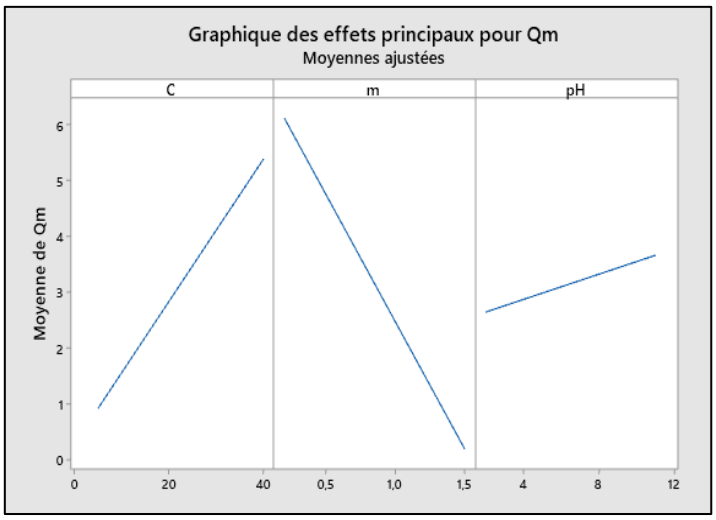

Figure 8: Main Effects Plot for Qm.
Source: Authors, (2026).

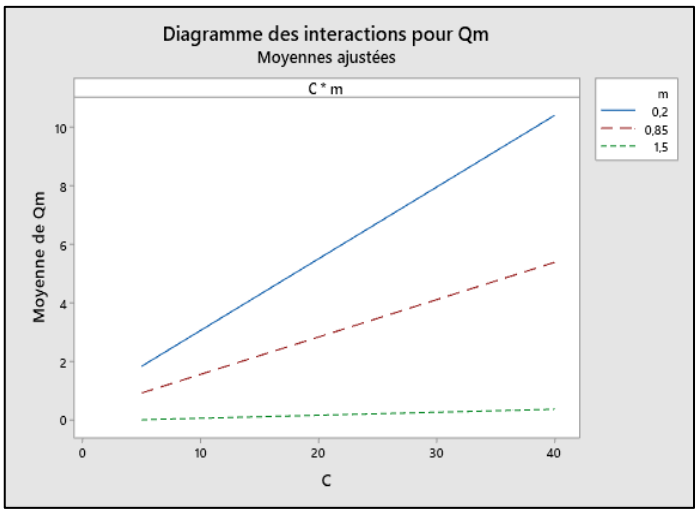

Figure 9: Interaction Plot between (C) and (m) for Qm.
Source: Authors, (2026).

III.4.1.4 Model Validation

The experimental conditions selected to validate the mathematical model are the upper levels of each factor:

Table 5: The experimental conditions chosen to validate the mathematical model are:

Variable	C	m	pH
Configuration	40	1,5	11

Source: Authors, (2026).

Under these conditions, the model estimated a response of Qm = 1.73436. To validate the mathematical model, a new experimental verification was conducted, yielding a result of Qm = 1.949714.

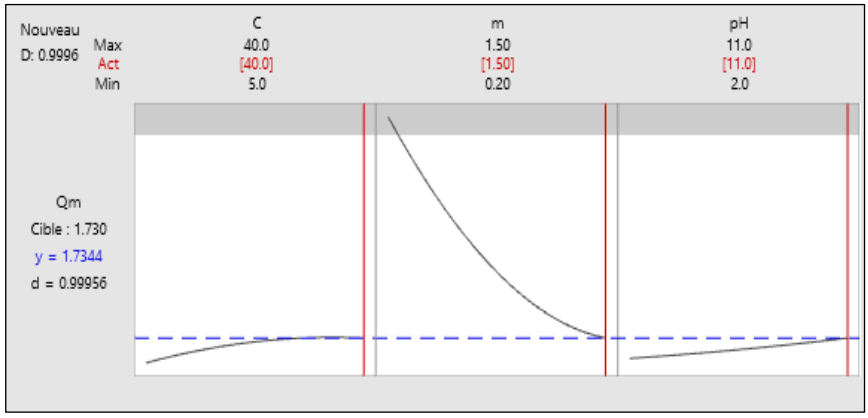

Figure 10: Estimation of the Response Qm at the High Level of Factors.
Source: Authors, (2026).

The desirability value (d = 0.999) is very close to 1, indicating that the model is well-validated and accurately predicts the adsorption behavior under the given conditions.

III.4.1.5 Response Surface Analysis

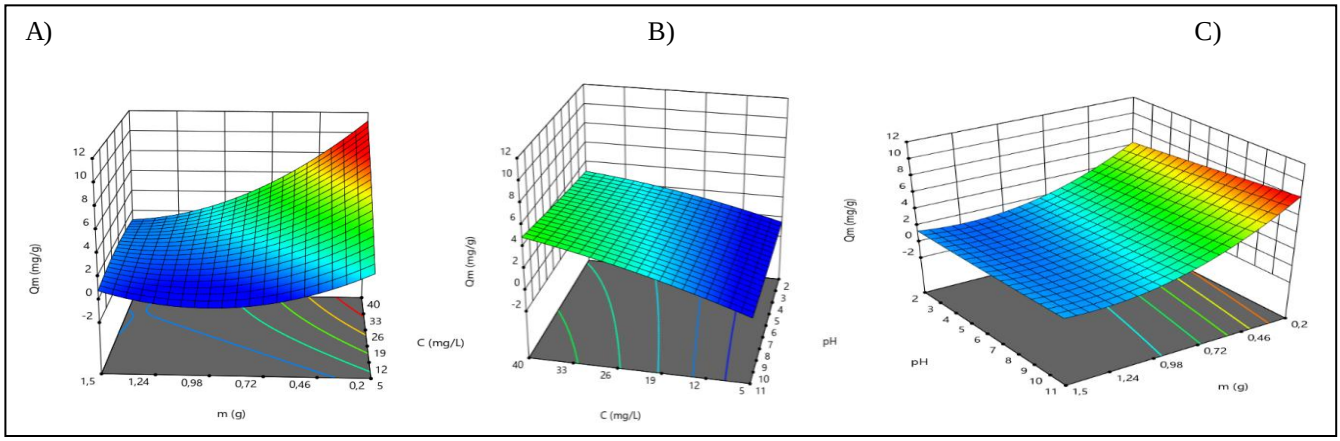

Figure 11: Response Surface Diagram Showing the Effect of each of two factors on Qm.
Source: Authors, (2026).

Figures 11, illustrate the effects of adsorbent mass, pH, and MB concentration on adsorption. Each figure shows the combined influence of two factors on the response (Qm), while the third factor is held constant at its midpoint.

III.4.2 Response Analysis of ΔC

III.4.2.1 Analysis of Variance (ANOVA)

Table 6: Analysis of Variance for the Qu adratic Response Surface Model for Concentration Variation.

Source	DF	Adjus Sum of Squares	CM adjust	F-value	P-value
Model	9	1403,11	155,90	45,33	0,000
Linear	3	1308,60	436,20	126,82	0,000
C	1	1207,44	1207,44	351,06	0,000
m	1	34,30	34,30	9,97	0,025
pH	1	66,85	66,85	19,44	0,007
Square Terms	3	16,18	5,39	1,57	0,307
C^2	1	11,03	11,03	3,21	0,133
m^2	1	1,13	1,13	0,33	0,591
pH^2	1	5,87	5,87	1,71	0,248
Two-Factor Interaction Terms	3	78,33	26,11	7,59	0,026
C×m	1	24,09	24,09	7,00	0,046
C×pH	1	54,07	54,07	15,72	0,011
m×pH	1	0,17	0,17	0,05	0,834
Error	5	17,20	3,44		
Lack of Fit	3	17,13	5,71	171,41	0,006
Pure Error	2	0,07	0,03		
Total	14	1420,31			

Source: Authors, (2026).

Table 7: Model Summary.

S	R Square	R Square (Adjus)	R Square (Predi)
1,93067	97,64%	96,33%	92,42%

Source: Authors, (2026).

According to Table 6, the model exhibited high significance, with a very low p-value ($p \leq 0.005$) as indicated by the ANOVA of the regression models. The linear effects, with a p-value of ≤ 0.0001, suggest a significant impact of the main factors (C, m, and pH), indicating that conversion varies based on these linear terms. Additionally, significant interaction effects were observed for C × m and C × pH. From the analysis of variance and the values in Table 11, the coefficient of determination (R^2 = 97.64%) and the adjusted R^2 (96.33%) are both close to 1, signifying that the model is well-fitted and accurately reflects the system's behavior. Furthermore, the predicted R^2 = 92.42% indicates a strong correlation between measured and predicted values. The effects are illustrated in the following Pareto chart.

III.4.2.2 Regression Equation In Uncoded Units

After excluding non-significant terms, the analysis of variance (ANOVA) shows that all remaining terms are highly significant, confirming that the refined model is statistically superior.

$$\Delta C = 4{,}82 + 0{,}215\,C - 1{,}67\,m - 0{,}48\,pH + 0{,}2157\,C \times m + 0{,}0467\,C \times pH$$

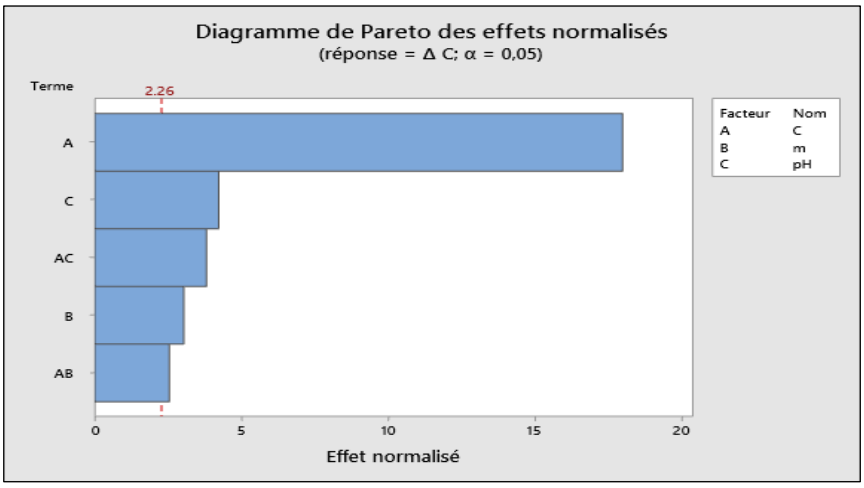

Figure 12: Pareto diagram of normalized effects for the response ΔC.
Source: Authors, (2026).

III.4.2.3 Main Effects and Interactions Affecting ΔC

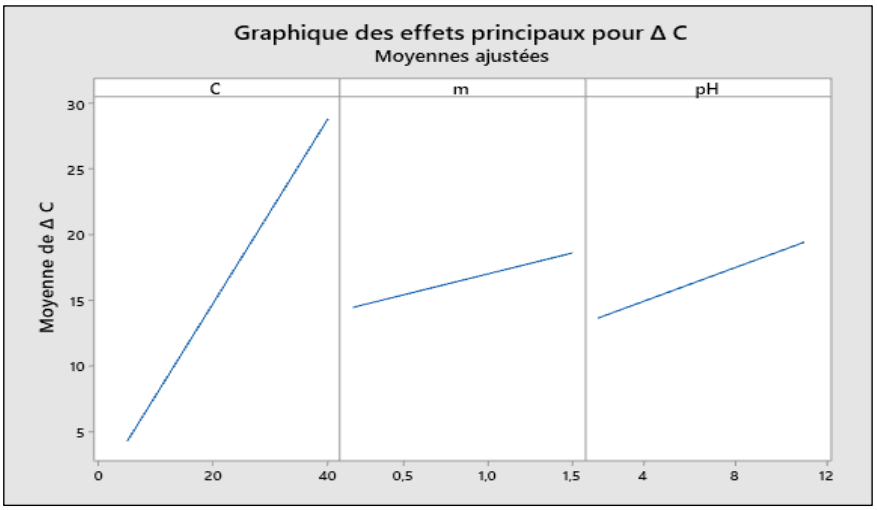

Figure 13: Main effects plot for ΔC.
Source: Authors, (2026).

According to Figure 13, we observe that the effect of all three factors is positive, and the effect of concentration is more significant than the effect of pH and mass (m).

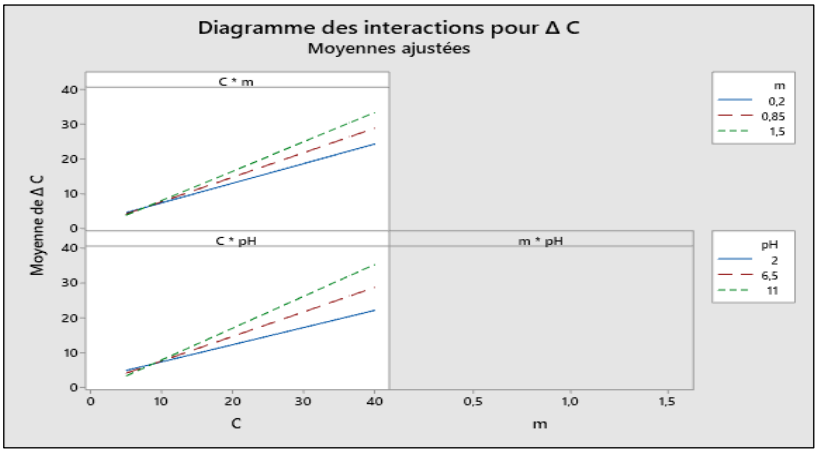

Figure 14: Interaction diagram for ΔC.
Source: Authors, (2026).

III.4.2.4 Model Validation

The conditions for ΔC obtained using the model at the high level were as follows:

Table 8: Experimental Conditions Chosen to Validate the Mathematical Model.

Variable	$C((\mathrm{mg/l}))$	$m\ (g)$	pH
Configuration	40	1,5	11

Source: Authors, (2026).

Under these conditions, the model estimated a response of ΔC = 38.06. To validate the model, a new experiment was conducted under identical conditions, yielding a result of ΔC = 37.81.

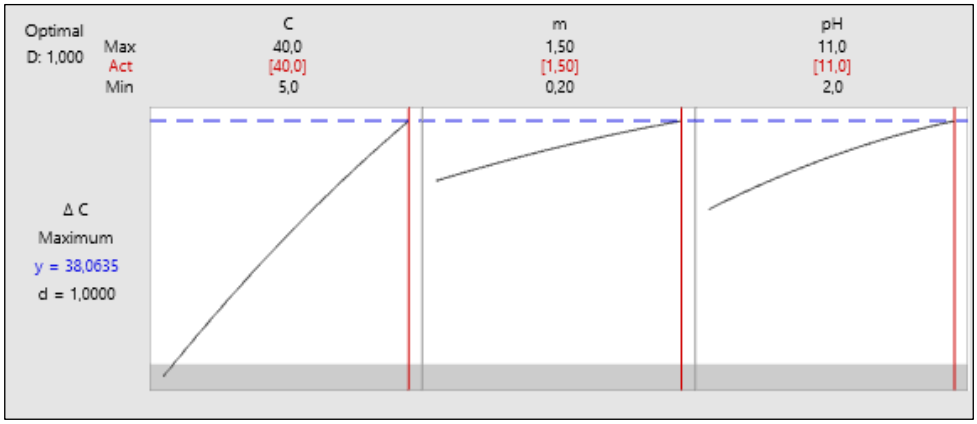

Figure 15: Optimization of the response ΔC.
Source: Authors, (2026).

III.4.2.5 Response Surface Analysis

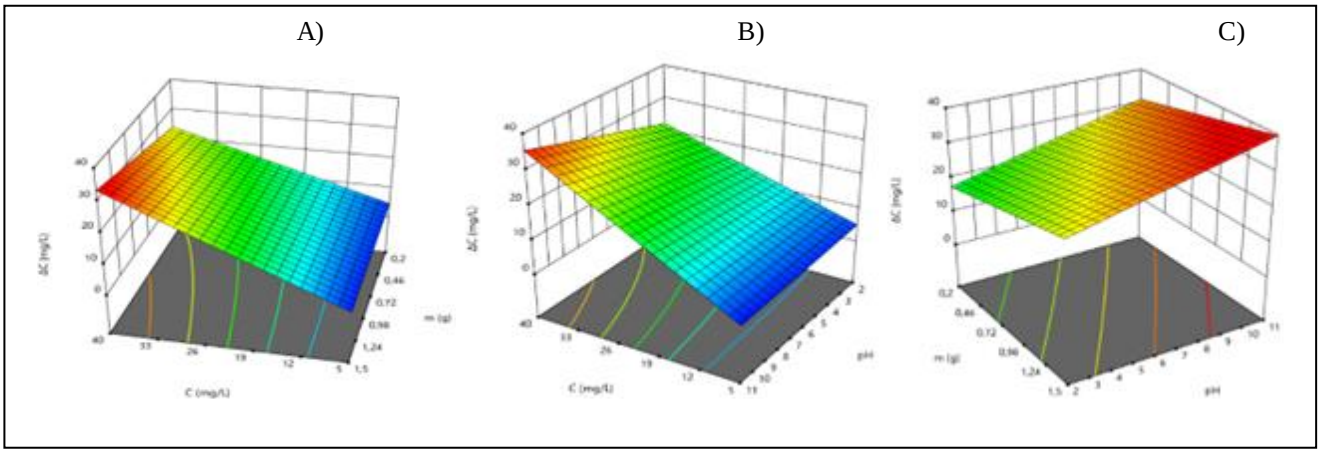

Figure 16: Response surface diagram showing the effect of each of two factors on ΔC.
Source: Authors, (2026).

Figures 16 show the effect of adsorbent mass, pH, and MB concentration on the response ΔC.

III.4.3 Response Analysis of R

Following the initial optimization of ΔC, we initiated a second experimental design to evaluate the yield by varying three factors: temperature, ionic strength (NaCl concentration), and agitation speed. The fixed factors are :

Table 9: Fixed Factors.

Waste Mass (g)	**MB Concentration (mg/l) |**	**pH**
1,5	40	11

Source: Authors, (2026).

III.4.3.1 Analysis of Variance (ANOVA)

Table 10: Analysis of Variance (ANOVA) for the Quadratic Response Surface Model for Yield (R).

Source	DF	Adjus Sum of Squares	CM adjust	F-value	P-value
Modèle	9	181,123	20,1248	107,54	0,000
Linéaires	3	145,693	48,5645	259,52	0,000
T	1	9,233	9,2331	49,34	0,001
C	1	51,320	51,3203	274,24	0,000
VA	1	85,140	85,1401	454,97	0,000
Square Terms	3	31,493	10,4978	56,10	0,000
T^2	1	1,300	1,2997	6,95	0,046
C^2	1	2,771	2,7714	14,81	0,012
VA^2	1	25,331	25,3308	135,36	0,000
Two-Factor Interaction Terms	3	3,936	1,3121	7,01	0,031
T×C	1	0,784	0,7837	4,19	0,096
T×VA	1	0,110	0,1100	0,59	0,478
C×VA	1	3,043	3,0427	16,26	0,010
Erreur	5	0,936	0,1871		
Lack of Fit	3	0,915	0,3050	29,61	0,033
Pure Error	2	0,021	0,0103		
Total	14	182,059			

Source: Authors, (2026).

Table 11: Model Summary.

S	R Square	R Square (Adjus)	R Square (Predi)
0,511223	99,00%	97,99%	95,07%

Source: Authors, (2026).

According to Table 10, the model is highly significant, as indicated by a very low p-value ($p \leq 0.0001$) from the ANOVA of the regression models. The linear effects, with a p-value of ≤ 0.0001, demonstrate a significant impact of the main factors (T, C, and VA), suggesting that conversion varies according to these linear terms. Additionally, a quadratic effect is observed for the squared term VA^2 ($p \leq 0.0001$), and a significant interaction effect is noted for C × VA. From the analysis of variance and the values in Table 16, the coefficient of determination (R^2 = 99.00%) and the adjusted R^2 (97.99%) indicate that the model fits well and accurately describe the system's behavior, as both values are close to 1. The predicted R^2 (95.07%) also indicates a strong correlation between the measured and predicted values. The effects are further illustrated in the accompanying Pareto chart.

III.4.3.2 Regression Equation In Uncoded Units

The analysis of variance (ANOVA), after excluding non-significant terms, shows that all remaining terms are highly significant. Thus, we conclude that the refined model is statistically superior.

$$R = 91{,}363 + 1{,}074\,T - 2{,}533\,C + 3{,}262\,VA + 0{,}593\,T^2 + 0{,}866\,C^2 - 2{,}619\,VA^2 + 0{,}872\,C \times VA$$

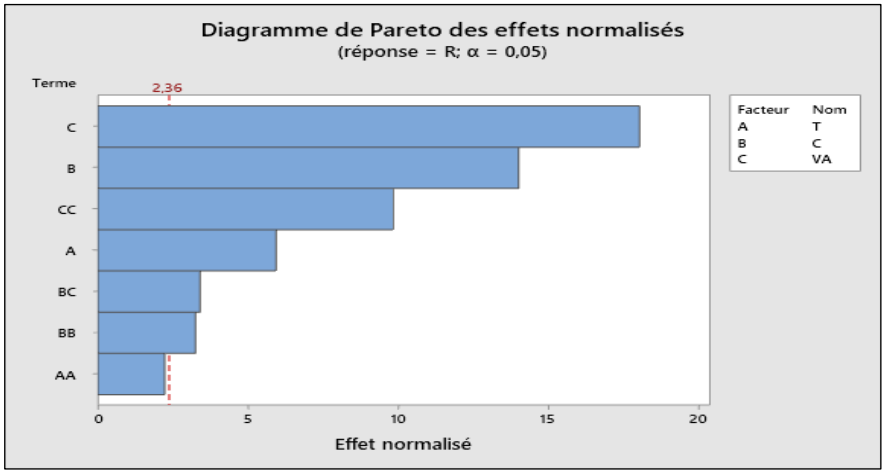

Figure 17: Pareto Chart of Normalized Effects for Response R.
Source: Authors, (2026).

III.4.3.3 Main Effects and Interactions Affecting R

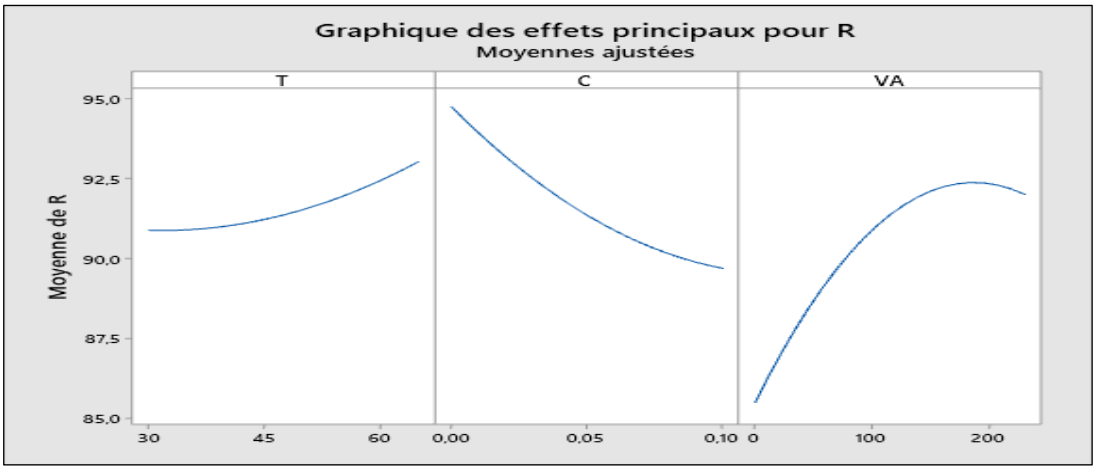

Figure 18: Main Effects Plot for Response R.
Source: Authors, (2026).

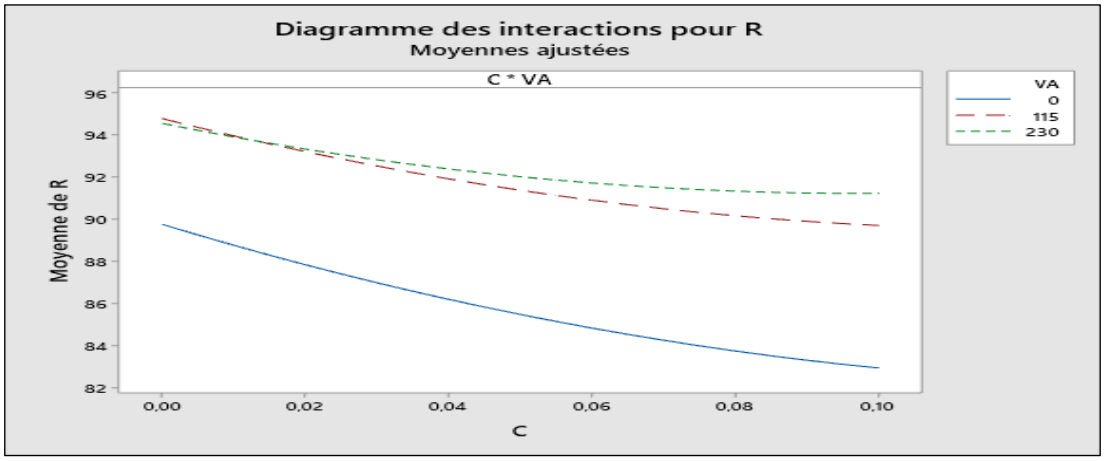

Figure 19: Interaction Diagrams for (Yield) R.
Source: Authors, (2026).

III.4.3.4 Model Validation

The conditions for R obtained using the model at the high level were as follows:

Table 12: The experimental conditions chosen to validate the mathematical model.

Variable	T(^{0}C)	C ((mg/l))	VA (r/m)
Configuration	65	0	167,273

Source: Authors, (2026).

Under these conditions, the model estimated a maximum response of R = 96.97. To validate the model, a new experimental verification was conducted under the same conditions, yielding a result of R = 96.78.

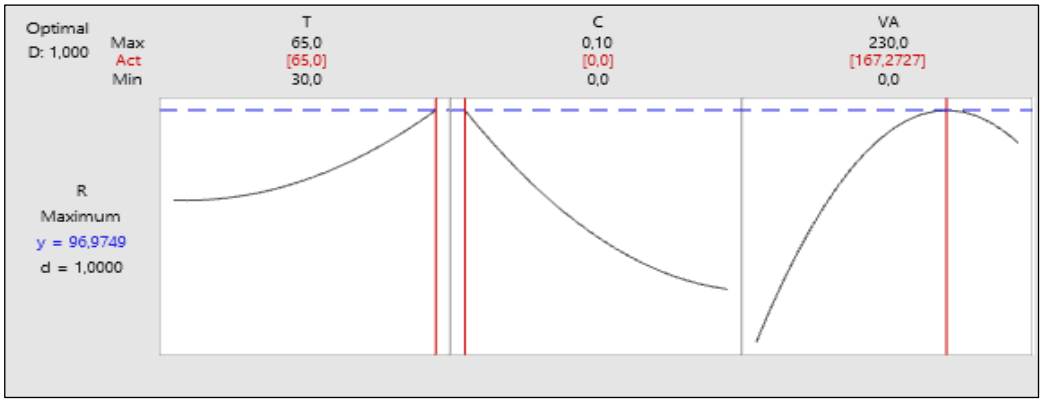

Figure 20: Optimization of the response R.
Source: Authors, (2026).

III.4.3.5 Response Surface Analysis

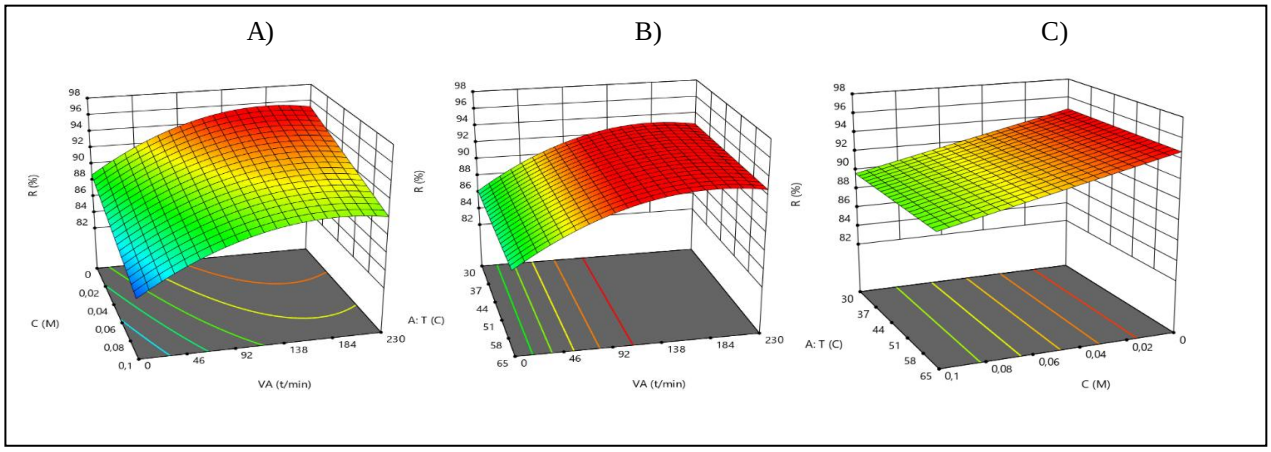

Figure 21: Response surface diagram showing the effect of each of two factors on R.
Source: Authors, (2026).

Figures 21 show the effect of the adsorbent mass, pH, and NaCl concentration on adsorption. Based on the two optimization experimental designs, the highest yield was achieved at the following factor levels:

Table 13 : Table of optimal values.

m(g)	C_{MB}(mg/l)	pH	VA	$C_{Na\ Cl}$(mg/l)	T(C°)
1.5	40	11	167,273	0	65

Source: Authors, (2026).

The value of pH has a very significant influence on the adsorption of MB. This is due to the effects of pH values on either the charges of the adsorbent's surface or the nature of MB Mall, Srivastava [5] . With low pH values, which correspond to high H^+ ion concentrations, the adsorbent particles acquire a net positive charge, resulting in a lack of attraction between the MB particles, which are also positive in nature. This, in turn, reduces the efficiency of MB adsorption onto activated carbon [6]. At higher pH values, where there is a lack of acidity in the environment, hence low H^+ ion concentration, a negative charge develops on the surface of activated carbon, which pulls MB particles due to their positive nature, hence increasing their adsorption [7]. Findings from studies show that the highest MB adsorption occurs in conditions of high pH values, with a peak in alkaline conditions [8] [9]. These findings correspond with our experiment results obtained from modeling. The amount of adsorbent used has an important role in determining the efficiency of MB dye adsorption.

With an increase in the amount of adsorbent, the number of adsorption sites also enhances, hence increasing the adsorption capacity owing to the enhanced surface area for binding of MB dye [10]. But beyond a point, an increase in the amount of adsorbent contributes little to the adsorption, as most of the adsorption sites are saturated [11]. Additionally, excess amount of adsorbent can cause a decrease in adsorption due to binding of particles, hence decreasing the surface area for adsorption. This has been supported by various studies related to MB dye adsorption [12].Water salinity has been shown to greatly influence MB adsorption due to changes in ionic strength in solutions. This means that higher water salinity, which contains ions from salts like NaCl, may lower MB adsorption efficiency [13]. Ions in dissolved salts increase competition for reactive sites on adsorbent surfaces, hence decreasing MB adsorption. Higher ionic strengths in solution also cause screening effects, which decrease adsorption between negatively charged adsorbent surfaces and MB chromophores due to reduced electrostatic interactions between MB and negatively charged adsorbents [14].

Stirring rate plays a significant role in the adsorption of methylene blue [2] dye, as it promotes mass transport between MB molecules and the adsorbent. Higher stirring rates can increase the rate of diffusion of MB molecules, which can also result in a thinner boundary layer around particles of adsorbent [15] with higher rates of adsorption. On the other hand, a stirring rate that is too high can lead to phenomena like particle agglomeration and MB desorption due to intensified turbulence, which in turn decreases adsorption efficiency [16].

Temperature plays a major role in influencing the adsorption of MB, in terms of both speed and capacity. Higher temperatures increase the molecular motion of the MB, hence increasing the rate of diffusion of MB towards the adsorption surface [17]. Higher temps also result in increased porosity of the adsorption surface, hence increasing its adsorption capacities due to higher available sites for adsorption [18]. Morphological analysis of the peanut shell was performed using scanning electron microscopy (SEM). At high magnification, the SEM micrographs revealed simple pitted cell walls with cave-like or porous structuresThe high adsorption efficiency is attributed to the peanut shell's spongy structure, which is rich in pores, facilitating the stabilization and retention of methylene blue within the material.

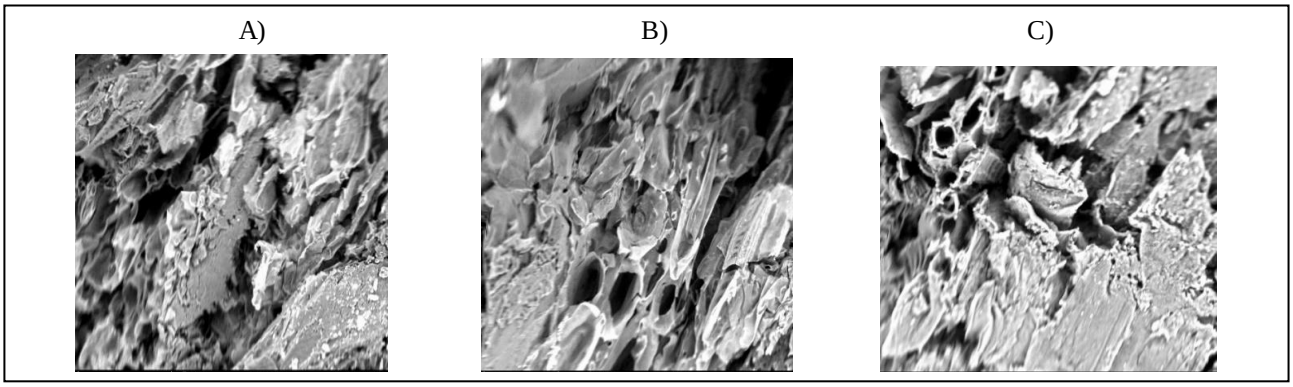

Figure 22: The morphological analysis of the peanut shell with SEM device before the adsorption process.
Source: Authors, (2026).

The following images were taken after the adsorption process and show the saturation of PS with MB.

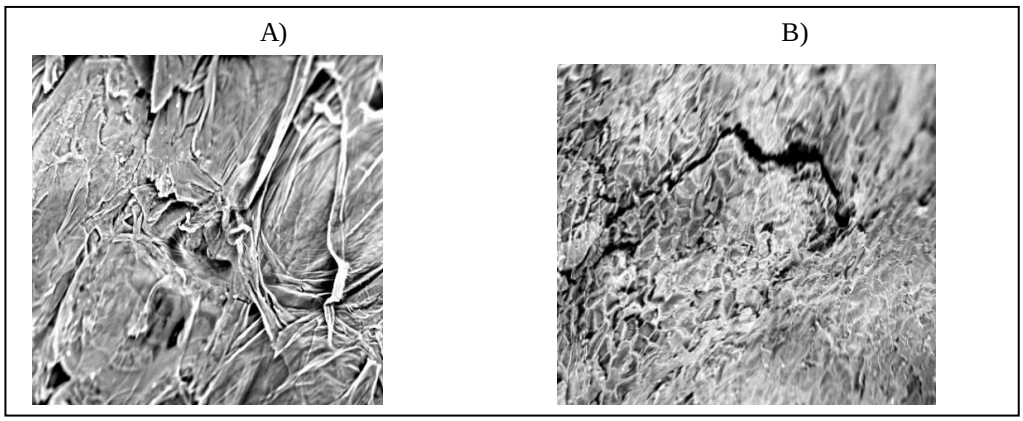

Figure 23: The morphological analysis of the peanut shell with SEM device after the adsorption process.
Source: Authors, (2026).

IV. CONCLUSIONS

The objective of this work is to study the elimination of methylene blue [2], which is a synthetic (cationic) dye present in textile industry effluents, by the adsorption technique. “Box-Behnken” is the experimental design adopted which facilitates our work to obtain the best adsorption efficiency, our results are as follows:

- The adsorption kinetics show that the adsorption process is very rapid and that equilibrium could be reached within the first 60 minutes.
- The modeling of adsorption isotherms using the Langmuir and Freundlich models shows that the Langmuir model better describes the experimental results.
- The kinetic study revealed that the adsorption process of methylene blue follows the pseudo-second-order model.
- Based on the validation of the two mathematical models with the following high-level factors: m = 1.5 g, C= 40 mg/L, and pH = 11 [2], we obtained experimental values of Qm and ΔC that are very close to the estimated values. This indicates that both mathematical models are well-fitted.
- The two experimental designs show that the yield of our study, obtained through the optimization of the response surface design "BOX-BEHNKEN," is better with the following five factors: adsorbent material mass 1.5 g, pH 11, temperature 65 °C, ionic strength concentration 0 mg/L, and stirring speed 167.273 rpm. These factors are used to achieve the maximum adsorption of methylene blue by the adsorbent (Peanut shells).
- By analyzing the two experimental designs, we achieved a yield of 97% through biosorption.

V. AUTHOR'S CONTRIBUTION

Conceptualization: Salah Eddine Bencheikh, Mohamed Bilal Goudjil and Ladjel Segni.
Methodology: Salah Eddine Bencheikh, Mohamed Bilal Goudjil and Ladjel Segni.
Investigation: Salah Eddine Bencheikh, Mohamed Bilal Goudjil and Ladjel Segni.
Discussion of results: Salah Eddine Bencheikh, Mohamed Bilal Goudjil and Ladjel Segni.
Writing – Original Draft: Salah Eddine Bencheikh.
Writing – Review and Editing: Salah Eddine Bencheikh, Mohamed Bilal Goudjil and Ladjel Segni.
Resources: Salah Eddine Bencheikh, Mohamed Bilal Goudjil and Ladjel Segni.
Supervision: Salah Eddine Bencheikh, Mohamed Bilal Goudjil and Ladjel Segni.
Approval of the final text: Salah Eddine Bencheikh, Mohamed Bilal Goudjil and Ladjel Segni.

VI. REFERENCES

[1] Adjaoud, S., Elimination d'un colorant anionique par un adsorpant naturel. 2018, UMMTO.

[2] Bouanimba, N. and R. Zouaghi, Modélisation et optimisation de la cinétique de dégradation photocatalytique de polluants organiques en solution aqueuse. 2009.

[3] Goupy, J. and L. Creighton, Introduction aux plans d'expériences-3ème édition-Livre+ CD-Rom. 2006: Hachette.

[4] Kimouche, K. and Z. Gheribi, Etude dequelques plans d'expériences associées aux surfaces de réponse. 2008, Université Frères Mentouri-Constantine 1.

[5] Mall, I.D., et al., Removal of Orange-G and Methyl Violet dyes by adsorption onto bagasse fly ash—kinetic study and equilibrium isotherm analyses. 2006. 69(3): p. 210-223.

[6] Gong, R., et al., Enhanced malachite green removal from aqueous solution by citric acid modified rice straw. 2006. 137(2): p. 865-870.

[7] Ahmad, R. and R.J.J.o.e.m. Kumar, Adsorption studies of hazardous malachite green onto treated ginger waste. 2010. 91(4): p. 1032-1038.

[8] Kumar, K.V. and S.J.J.o.h.m. Sivanesan, Comparison of linear and non-linear method in estimating the sorption isotherm parameters for safranin onto activated carbon. 2005. 123(1-3): p. 288-292.

[9] Mittal, A., J. Mittal, and L.J.J.o.h.m. Kurup, Adsorption isotherms, kinetics and column operations for the removal of hazardous dye, Tartrazine from aqueous solutions using waste materials—Bottom Ash and De-Oiled Soya, as adsorbents. 2006. 136(3): p. 567-578.

[10] Gong, R., et al., Utilization of powdered peanut hull as biosorbent for removal of anionic dyes from aqueous solution. 2005. 64(3): p. 187-192.

[11] Malik, P.K.J.D. and pigments, Use of activated carbons prepared from sawdust and rice-husk for adsorption of acid dyes: a case study of Acid Yellow 36. 2003. 56(3): p. 239-249.

[12] Crini, G.J.B.t., Non-conventional low-cost adsorbents for dye removal: a review. 2006. 97(9): p. 1061-1085.

[13] Malik, P.J.J.o.H.M., Dye removal from wastewater using activated carbon developed from sawdust: adsorption equilibrium and kinetics. 2004. 113(1-3): p. 81-88.

[14] Aljeboree, A.M., A.N. Alshirifi, and A.F.J.A.j.o.c. Alkaim, Kinetics and equilibrium study for the adsorption of textile dyes on coconut shell activated carbon. 2017. 10: p. S3381-S3393.

[15] Mohan, D. and C.U.J.J.o.h.m. Pittman Jr, Activated carbons and low cost adsorbents for remediation of tri-and hexavalent chromium from water. 2006. 137(2): p. 762-811.

[16] Salleh, M.A.M., et al., Cationic and anionic dye adsorption by agricultural solid wastes: a comprehensive review. 2011. 280(1-3): p. 1-13.

[17] Tan, I., A.L. Ahmad, and B.H.J.D. Hameed, Adsorption of basic dye using activated carbon prepared from oil palm shell: batch and fixed bed studies. 2008. 225(1-3): p. 13-28.

[18] Bhattacharyya, K.G., S.S.J.A.i.c. Gupta, and i. science, Adsorption of a few heavy metals on natural and modified kaolinite and montmorillonite: a review. 2008. 140(2): p. 114-131.